Current patterns in the phonon-maxon-roton excitations in ^{4}He

V. Apaja and M. Saarela
Department of Physical Sciences/Theoretical Physics, University of Oulu, SF-90570 Oulu, Finland
(Received 23 July 1997)

The structure of one- and two-particle currents in liquid ^{4}He in the region of the phonon, maxon, and roton excitations is calculated using linear-response theory. A set of continuity equations is derived from the minimal-action principle. The two-particle current describes the motion of the ^{4}He atoms with respect to each other and thus enables us to identify topological structures. The optimized functional space makes no assumptions on the patterns and we show how a simple sound wave of the phonon excitation develops into an atomic-size backflow roll above the roton minimum at wave numbers $k \geqslant 2.5$ Å^{-1}. The roll gets elongated in the direction of the center-of-mass motion and forms a tubelike structure of atomic diameter when $k \geqslant 3.0$ Å^{-1}. The roton minimum itself is a resonance effect where the wavelength of the excitation matches with the wavelength of the oscillations caused by the two-particle correlations. [S0163-1829(98)00109-X]

I. INTRODUCTION

The elementary excitation spectrum of the strongly correlated ^{4}He liquid is experimentally well established.[1,2] Historically different parts of the spectrum have names; phonon refers to the linear long-wavelength part, maxon to the region around the maximum, and roton to the region around the minimum. Microscopic structures of the maxon and roton excitations are still under active discussion.[3–7] Feynman originally suggested that *backflow* currents[8,9] are necessary to conserve the total current. He assumed that these currents behave like a smoke ring. Williams then followed the Onsager-Feynman idea of vortex excitations[10,11] and made a specific assumption that the backflow currents are three-dimensional vortex rings with vorticity equal to one and the minimum radius of the ring is the radius of a ^{4}He atom. Parameters of the model were fixed in such a way that the energy of a minimum size vortex ring is equal to the energy of the roton minimum. In more microscopic approaches[3,7,4] the starting point is the variational wave function. Galli *et al.*[3] used the shadow wave function with an explicit backflow term and calculated the excitation spectrum in the maxon-roton region which agreed well with experimental results near the roton minimum. In their approach no vorticity quantum number is associated with the roton excitation and they conclude that at the roton minimum the local density and momentum coincide with those of a single-particle excitation.

In this work we study the structure of elementary excitations using the linear-response theory and the minimal-action principle.[7,12,4] We assume that the fluid is driven by a weak external disturbance with a given frequency and wave number,

$$U_{\mathrm{ext}}(\mathbf{r};t) = \tilde{U}_{\mathrm{ext}}(k,\omega) e^{i(\mathbf{k}\cdot\mathbf{r}+\omega t)}, \tag{1}$$

and calculate the one- and two-particle currents from the continuity equations. The one-particle current is simply the phase velocity times the density fluctuation, but the two-particle current determines how atoms move with respect to each other and thus shows the flow patterns.

II. THEORY

The dynamic, variational theory of excitations in liquid ^{4}He starts from the action integral

$$\mathcal{L}(t) = \int_{t_0}^{t} dt \left\langle \Phi(t) \left| H - i\hbar \frac{\partial}{\partial t} \right| \Phi(t) \right\rangle, \tag{2}$$

which contains the Hamiltonian

$$H = -\frac{\hbar^2}{2m} \sum_{i=1}^{N} \nabla_i^2 + \sum_{i<j=1}^{N} V(|\mathbf{r}_i - \mathbf{r}_j|) + \sum_{i=1}^{N} U_{\mathrm{ext}}(\mathbf{r}_i;t), \tag{3}$$

where the two-particle interaction is chosen to be the Aziz potential.[13]

The variational wave function,

$$\Phi(\mathbf{r}_1, \ldots, \mathbf{r}_N;t) = \frac{1}{\mathcal{N}} e^{-iEt/\hbar} e^{(1/2)\delta U(t)} \Psi(\mathbf{r}_1, \ldots, \mathbf{r}_N), \tag{4}$$

is a product of three terms, the optimized wave function of the ground state $\Psi(\mathbf{r}_1, \ldots, \mathbf{r}_N)$, a *kinematic* phase factor and a *dynamic* complex function $\exp(\frac{1}{2}\delta U(t))$, divided with the normalization factor $\mathcal{N} = \int d\tau \Psi^2 e^{\mathrm{Re}[\delta U(t)]}$. The function $\delta U(t)$ describes fluctuations in the correlation functions due to the external disturbance,

$$\delta U(t) = \sum_i \delta u_1(\mathbf{r}_i;t) + \sum_{i<j} \delta u_2(\mathbf{r}_i, \mathbf{r}_j;t). \tag{5}$$

We include the time dependence in both one- and two-particle correlation functions. If only $\delta u_1(\mathbf{r}_i;t)$ is included one obtains the Feynman spectrum.[8]

The variation of the action integral with respect to $\delta u_1(\mathbf{r}_1;t)$ and $\delta u_2(\mathbf{r}_1, \mathbf{r}_2;t)$ leads to linearized one- and two-particle continuity equations, respectively,[7,12]

$$\nabla_1\cdot\mathbf{j}_1(\mathbf{r}_1;t)+\delta\dot{\rho}_1(\mathbf{r}_1;t)=D_1(\mathbf{r}_1;t),$$

$$\nabla_1\cdot\mathbf{j}_2(\mathbf{r}_1,\mathbf{r}_2;t)+\delta\dot{\rho}_2(\mathbf{r}_1,\mathbf{r}_2;t)+(1\leftrightarrow 2)=D_2(\mathbf{r}_1,\mathbf{r}_2;t), \tag{6}$$

with the time-dependent parts of the one- and two-particle densities $\delta\dot{\rho}_1(\mathbf{r}_1;t)$ and $\delta\dot{\rho}_2(\mathbf{r}_1,\mathbf{r}_2;t)$, and the currents

$$\mathbf{j}_1(\mathbf{r}_1;t)=\frac{\hbar\overline{\rho}}{2mi}\Big[\nabla_1\delta u_1(\mathbf{r}_1;t)+\overline{\rho}\int d^3r_2 g(|\mathbf{r}_1-\mathbf{r}_2|)\times\nabla_1\delta u_2(\mathbf{r}_1,\mathbf{r}_2;t)\Big],$$

$$\mathbf{j}_2(\mathbf{r}_1,\mathbf{r}_2;t)=\frac{\hbar\overline{\rho}^2}{2mi}\Big[g(|\mathbf{r}_1-\mathbf{r}_2|)\nabla_1[\delta u_1(\mathbf{r}_1;t)+\delta u_2(\mathbf{r}_1,\mathbf{r}_2;t)]+\overline{\rho}\int d^3r_3 g_3(\mathbf{r}_1,\mathbf{r}_2,\mathbf{r}_3)\nabla_1\delta u_2(\mathbf{r}_1,\mathbf{r}_3;t)\Big]. \tag{7}$$

Here $\overline{\rho}$ is the density of the ground state, m is the mass of the ^{4}He atom, $g(|\mathbf{r}_1-\mathbf{r}_2|)$ is the radial distribution function of the ground state, and $g_3(\mathbf{r}_1,\mathbf{r}_2,\mathbf{r}_3)$ is the ground-state triplet distribution function related to the three-particle density by $\rho_3(\mathbf{r}_1,\mathbf{r}_2,\mathbf{r}_3)=\overline{\rho}^3 g_3(\mathbf{r}_1,\mathbf{r}_2,\mathbf{r}_3)$.

Since the external disturbance drives the fluid with a given frequency and wave number defined in Eq. (1) both $\delta\rho_1(\mathbf{r}_1;t)$ and $\delta u_1(\mathbf{r}_1;t)$ fluctuate in phase with that. Fluctuations of the two-particle density are more complicated and come out as a solution of the continuity equations. The driving terms D_1 and D_2 are proportional to the external disturbance and their expressions are found in Ref. 7.

The exact Born-Green-Yvon (BGY) equations connect the gradients of the correlation functions and densities. Keeping only the linear terms in the fluctuations of these quantities we can write the currents entirely in terms of the density fluctuations

$$\mathbf{j}_1(\mathbf{r}_1;t)=\frac{\hbar}{2mi}\Big[\nabla_1\delta\rho_1(\mathbf{r}_1;t)-\int d\mathbf{r}_2\delta\rho_2(\mathbf{r}_1,\mathbf{r}_2;t)\times\nabla u_2(|\mathbf{r}_1-\mathbf{r}_2|)\Big], \tag{8}$$

$$\mathbf{j}_2(\mathbf{r}_1,\mathbf{r}_2;t)=\frac{\hbar}{2mi}\Big[\nabla_1\delta\rho_2(\mathbf{r}_1,\mathbf{r}_2;t)-\delta\rho_2(\mathbf{r}_1,\mathbf{r}_2;t)\times\nabla_1 u_2(|\mathbf{r}_1-\mathbf{r}_2|)-\int d\mathbf{r}_3\delta\rho_3(\mathbf{r}_1,\mathbf{r}_2,\mathbf{r}_3;t)\times\nabla_1 u_2(|\mathbf{r}_1-\mathbf{r}_3|)\Big], \tag{9}$$

where $u_2(|\mathbf{r}_1-\mathbf{r}_2|)$ is the two-particle correlation function of the ground state. Since only the exact definitions are used the currents satisfy the sequential condition $\int d\mathbf{r}_2\mathbf{j}_2(\mathbf{r}_1,\mathbf{r}_2;t)=(N-1)\mathbf{j}_1(\mathbf{r}_1;t)$.

We calculate the currents created at the frequencies and wave numbers of the lowest excitation modes where the linear-response function,

$$\chi(k,\omega)=\frac{\delta\rho(k,\omega)}{\widetilde{U}_{\rm ext}(k,\omega)} \tag{10}$$

has poles. That is done by taking the Fourier transform of the continuity equations (6) and searching for the solutions where the driving terms D_1 and D_2 are equal to zero.

The functional space in the minimization of the action integral is limited to the fluctuating one- and two-particle correlations in Eq. (5). A similar approximation was also used in the Feynman-Cohen wave function[9]

$$\phi_F=\Psi\sum_l e^{i\mathbf{k}\cdot\mathbf{r}_l}e^{i\Sigma_{j\neq l}\kappa(|\mathbf{r}_j-\mathbf{r}_l|)}. \tag{11}$$

On the other hand, we do not make any parametrized assumptions of the backflow patterns and thus their appearance is determined by the continuity equations.

The second approximation concerns the fluctuations of the triplet distribution function in Eq. (9). Here we also follow the approach taken by Feynman and Cohen and use the superposition approximation, $\rho_3(\mathbf{r}_1,\mathbf{r}_2,\mathbf{r}_3)=\overline{\rho}^3 g(\mathbf{r}_1,\mathbf{r}_2)g(\mathbf{r}_2,\mathbf{r}_3)g(\mathbf{r}_1,\mathbf{r}_3)$. Linear fluctuations in ρ_3 can then be expressed as a sum of fluctuations in the radial distribution functions. Thirdly, we have to evaluate the gradient of the two-particle correlation function in the ground state. That can be expressed entirely in terms of the radial distribution function or the structure function $S(k)$ in the momentum space by using the hypernetted chain equations $g(r)\nabla u_2(r)=\nabla[X(r)-E(r)]-(g(r)-1)\nabla[N(r)+E(r)]$. Here $X(r)$ is the direct correlation function, $N(r)$ is the sum of nodal diagrams, and $E(r)$ is the sum of elementary diagrams.[14,15]

III. RESULTS

The input into the continuity equations is the static structure function $S(k)$ of the ground state. It can be taken from experiments or from theoretical calculations. We have tested the sensitivity of the results by using the measured $S(k)$ of Ref. 16 and the one from our variational ground-state calculation[14] (see Fig. 1). The resulting spectra differ somewhat in the maxon-roton region. When the experimental $S(k)$ is used the roton minimum is at $k=1.93$ Å^{-1} with the energy 8.74 K and the maxon maximum at $k=1.19$ Å^{-1} with the energy 13.80 K. That compares very well with different experiments.[2] Woods *et al.*[17] find the roton minimum at $k=1.926\pm0.005$ Å^{-1} with the energy 8.618 ± 0.009 K and Svensson *et al.*[18] find the maxon peak at $k=1.13$ Å^{-1} with the energy 13.82 K. The agreement suggests that right physical ingredients are included in our approximations. Since the peak of the variational structure function is slightly lower and at a slightly higher k than the experimental one the use of variational $S(k)$ moves the roton minimum to the energy 9.16 K at 1.98 Å^{-1} and raises the maxon peak to 14.85 K at 1.21 Å^{-1}. At wave numbers $k>2.5$ Å^{-1} we find the flattening of the dispersion relation due to opening of the decay channel into two rotons.[3,19] The comparison of the full, calculated excitation spectra with experiments is shown in Fig. 1. We have also calculated the strength of the pole, $Z(k)$, of the elementary excitation, in the dynamic structure function $S(k,\omega)$. That gives a more stringent test than the excitation

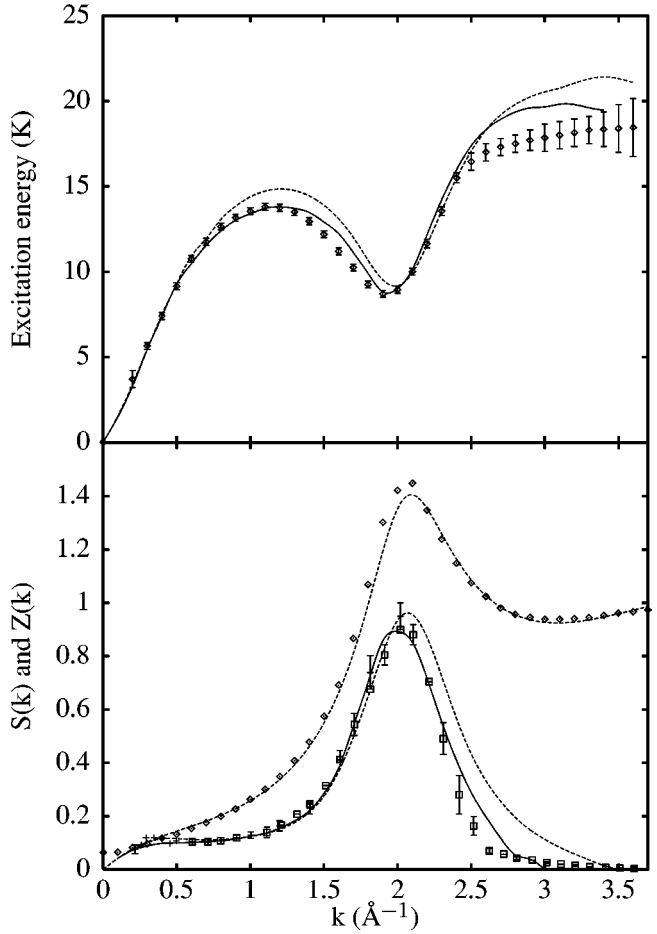

FIG. 1. In the upper figure we show the elementary excitation spectra calculated from the present theory using the measured structure function from Ref. 16 (full line) and the calculated structure function from Ref. 14 (dashed line). The diamonds with error bars give the measured spectrum of Ref. 1. The structure function $S(k)$ and the strength of the elementary excitations $Z(k)$ are shown in the lower figure. The diamonds are the results from the experiments of Ref. 16 for $S(k)$ and the squares and crosses for the $Z(k)$ from Ref. 1. The solid line is the calculated result for $Z(k)$ using the experimental $S(k)$, the upper dashed line is the calculated $S(k)$ and the lower one the corresponding $Z(k)$.

spectrum to the solution of the continuity equations. The results agree very well with experiments for the full range of wave numbers as shown also in Fig. 1.

From the continuity equations we also solve the *local*-density fluctuations and the currents at wave numbers and frequencies along the elementary excitation curve. The one-particle current,

$$\mathbf{j}_1(k;\omega)=\frac{\omega}{k}\delta\rho_1(k,\omega), \tag{12}$$

is proportional to the phase velocity, in the long-wavelength limit that is determined by the speed of sound.

We have chosen to present our results for the real part of the two-particle current of Eq. (9) in the mixed representation as a function of center-of-mass momentum and relative coordinate. It can then be written in the form

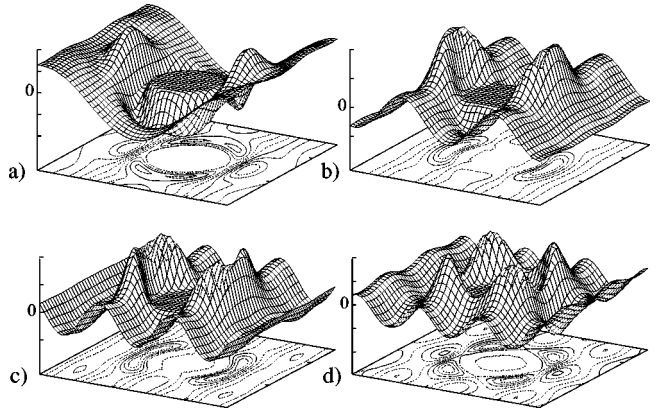

FIG. 2. The z component of the two-particle current (a) at the maxon region $k=1.0$ Å^{-1}, (b) near the roton minimum $k=2.0$ Å^{-1}, (c) at $k=2.5$ Å^{-1}, and (d) in the asymptotic region $k=3.0$ Å^{-1}. The direction of $\mathbf{k}$ is along x axis.

$$\mathbf{j}_2(\mathbf{k},\mathbf{r},\omega)=\overline{\rho g(r)}\left[\mathbf{j}_1(\mathbf{k},\omega)\cos\left(\frac{1}{2}\mathbf{k}\cdot\mathbf{r}\right)+\frac{\hbar\overline{\rho}}{2mi}\widetilde{\mathbf{T}}(\mathbf{k},\mathbf{r},\omega)\right]. \tag{13}$$

The radial distribution function of the ground state $g(r)$ gives the probability of finding another particle at the distance r away from a given particle. We locate particle one into the origin and because of the repulsive core of the interaction other particles are repelled outside the radius of about 2 Å. This ''correlation hole'' is clearly seen in Figs. 2 and 3.

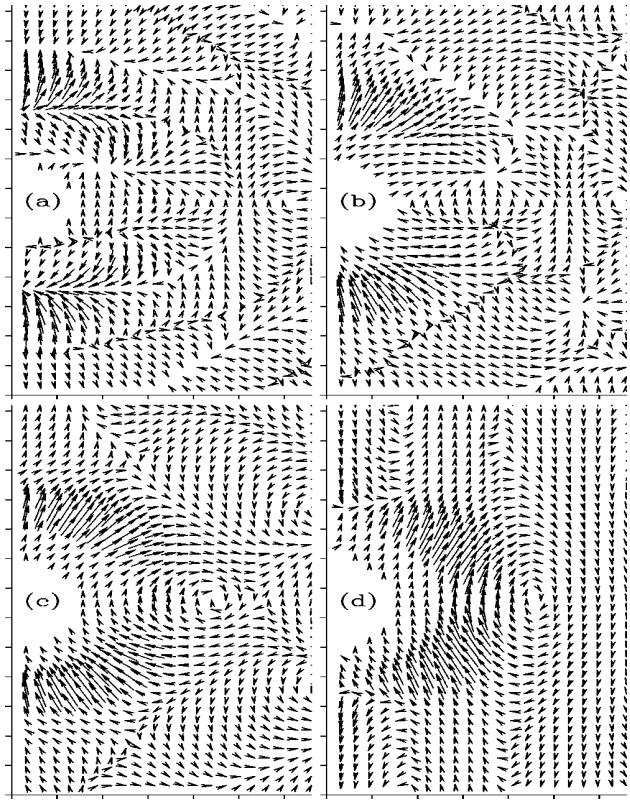

FIG. 3. The short-range part of the two-particle current (a) at the maxon region $k=1.0$ Å^{-1}, (b) near the roton minimum $k=2.0$ Å^{-1}, (c) at $k=2.5$ Å^{-1}, and (d) in the asymptotic region $k=3.0$ Å^{-1}. The center-of-mass oscillations have been subtracted. The direction of $\mathbf{k}$ is upwards and the tickmark spacing is 1 Å.

We also separate out the oscillating behavior of the sound-like wave where particles move towards each other and away from each other with the wavelength determined by the center-of-mass motion in the cosine term. The more complicated flow patterns are collected into $\tilde{\mathbf{T}}(\mathbf{k},\mathbf{r},\omega)$. The coordinate system is such that the center-of-mass momentum points to the z direction.

In Fig. 2 we have plotted the z component of the two-particle current in four typical cases of the center-of-mass motion with the wave numbers $k=1.0$ Å^{-1} (maxon), 2.0 Å^{-1} (roton), 2.5 and 3.0 Å^{-1} (the asymptotic region). Besides the center-of-mass oscillations there are oscillations due to interparticle correlations. The most pronounced in Fig. 2 is the nearest neighbor peak. From Fig. 2(a) one can see that in the maxon region these two kinds of oscillations are out of phase whereas in the roton region of Fig. 2(b) they are in phase. That is why the roton region is energetically favored and the minimum corresponds to the wave number of the peak of the structure function $S(k)$. This is already well known from the Feynman spectrum $\hbar^2k^2/2mS(k)$. When the wavelength becomes shorter than the size of the correlation hole the simple wave pattern breaks down [see Figs. 2(c) and 2(d)].

A more detailed structure of the current flow is shown in Fig. 3 where we have subtracted the center-of-mass oscillations. The current flows to the direction of arrows and since it has cylindrical symmetry we show only the $x-z$ plane with $x\geqslant 0$. In the maxon and roton regions [Figs. 3(a) and 3(b)] the dominant feature is the oscillation of the radial distribution function, though some interesting topological structures could be identified. The pattern, however, changes completely at 2.5 Å^{-1}. A clear backflow loop is formed around each atom in Fig. 3(c). The radius of the circulation is of the order of atomic radius (compare with the white area in the figures). When $k>2.5$ Å^{-1} the loop gets elongated with increasing wave number and forms a tubelike structure with a diameter of atomic size. A typical case at 3.0 Å^{-1} is shown in Fig. 3(d).

IV. SUMMARY

As a summary we have shown that the linear-response theory based on the time-dependent variational wave function gives very good results for the elementary excitation spectrum and its strength in $S(k,\omega)$. The equations of motion which minimize the action integral enable us to calculate the one- and two-particle currents. The one-particle current is proportional to the phase velocity, whereas the two-particle current shows the flow patterns of the relative motion between ^{4}He atoms. At the roton minimum the size of the correlation hole created by an atom matches with the wavelength of the center-of-mass motion. The topological structure of the two-particle current shows a complicated pattern of atomic size, but no backflow motion is visible. The backflow rolls, like smoke rings, appear at short wavelengths when $k\geqslant 2.5$ Å^{-1} and get elongated into tubes with decreasing wavelengths.

In our wave function we have not put in quantized vortices[20,21] and the structures seen in Figs. 3(c) and 3(d) come out of the full optimization of the action integral with respect to the fluctuating one- and two-particle correlation functions. They do not carry any conserved vorticity quantum number. The relation between these excitations and the vortex excitations will be investigated further.

ACKNOWLEDGMENTS

It gives us pleasure to thank Eckhard Krotscheck, Fyodor Kusmartsev, and Charles Campbell for many stimulating discussions and the Academy of Finland for financial support.

[1] R. A. Cowley and A. D. B. Woods, Can. J. Phys. **49**, 177 (1971).
[2] R. J. Donnelly, J. A. Donnelly, and R. N. Hills, J. Low Temp. Phys. **44**, 471 (1981).
[3] D. E. Galli, E. Cecchetti, and L. Reatto, Phys. Rev. Lett. **77**, 5401 (1996).
[4] B. E. Clements, E. Krotscheck, and C. J. Tymczak, Phys. Rev. B **53**, 12 253 (1996).
[5] M. Boninsegni and D. M. Ceperley, J. Low Temp. Phys. **104**, 339 (1996).
[6] G. A. Williams, Phys. Rev. Lett. **68**, 2054 (1992).
[7] M. Saarela and J. Suominen, in *Condensed Matter Theories*, edited by J. Keller (Plenum, New York, 1989), Vol. 4, p. 377.
[8] R. P. Feynman, Phys. Rev. **94**, 262 (1954).
[9] R. P. Feynman and M. Cohen, Phys. Rev. **102**, 1189 (1956).
[10] L. Onsager, Nuovo Cimento Suppl. **6**, 249 (1949) (discussion on a paper by C. J. Gorter).
[11] R. P. Feynman, in *Progress in Low Temperature Physics*, edited by C. J. Gorter (North-Holland, Amsterdam, 1955), Vol. I, Chap. 2.
[12] B. E. Clements *et al.*, Phys. Rev. B **50**, 6958 (1994).
[13] R. A. Aziz *et al.*, J. Chem. Phys. **70**, 4330 (1979).
[14] E. Krotscheck and M. Saarela, Phys. Rep. **232**, 1 (1993).
[15] Detailed evaluation of $g(r)\nabla u_2(r)$ will be given in the forthcoming paper.
[16] H. N. Robkoff and R. B. Hallock, Phys. Rev. B **24**, 159 (1981).
[17] A. D. B. Woods, P. A. Hilton, R. Scherm, and W. G. Stirling, J. Phys. C **10**, L45 (1977).
[18] E. C. Svensson, R. Scherm, and A. D. B. Woods, J. Phys. (Paris) Colloq. **39**, C6-211 (1978).
[19] V. Apaja *et al.*, Phys. Rev. B **55**, 12 925 (1997).
[20] M. Saarela and F. V. Kusmartsev, Phys. Lett. A **202**, 317 (1995).
[21] S. Giorgini, J. Boronat, and J. Casulleras, Phys. Rev. Lett. **77**, 2754 (1996).